TITAN: DETERMINATION OF THE LOCAL TECTONIC FIELD AT THE TITAN LAKE OBSERVED FROM THE CASSINI FLYBY ON FEBRUARY 22, 2007

Georgios Bampasidis [1], Athena Coustenis [2], Xenophon Moussas [1]

[1] *Department of Astrophysics, Astronomy and Mechanics, Faculty of Physics, National & Kapodistrian University of Athens, Panepistimiopolis, GR 15783, Zographos, Athens, Greece,*
Email: gbabasid@phys.uoa.gr, xmoussas@phys.uoa.gr
[2] *LESIA, Observatoire de Paris-Meudon, 92195, Meudon, Cedex, France,*
Email: athena.coustenis@obspm.fr

ABSTRACT

Images from the Huygens' descending phase revealed different and strange features on Titan's surface such as craters, dunes, volcanoes, ridges, rivers, lakes, mountains, etc. Moreover, the Cassini orbiter is executing 45 flybys of Titan, so more details are certain to appear. During a near-polar flyby on February 22, 2007 the Cassini's radar instrument, showed a big island or a peninsula in the middle of one of the largest hydrocarbon lakes imaged on Titan. We consider here the interaction between the local tectonic field and atmospheric phenomena, which can shape this island by studying its drainage.
The main attribute of this work is to quantify the hierarchy of stream segments according to the ordering classification system proposed by Horton & Strahler in the observed drainage. In this system, the channel segment, which begins from the head of the stream, is assigned the value 1 and called first-order stream. When two first-order streams come together, they form a second-order stream, two second order streams formed a third order stream, and so on. After having measured the length of the stream segments and its basins, it is possible to estimate the liquid budgets of this drainage and the hydrocarbon lake supply.
Analysis of this data reveals some interesting aspects of vertical tectonic movements of the area. In addition, the measurement of drainage density provides a useful numerical measure of landscape dissection and runoff potential.
We present these considerations in the framework of future space missions to Titan with an orbiter. Higher resolution images from a laser or radar altimeter on board are required to better define the estimated measurements.

1. INTRODUCTION

Titan, the largest moon of Saturn, is revealing scientists its surface, thanks to the Cassini's orbiter fly-bys since 2004 and the 2005 *in situ* Huygens' probe measurements. Similarly to Earth's features, craters, dunes, volcanoes, ridges, lakes, mountains, channels and rivers appear in the Cassini-Huygens mission's observations [2, 11, 12].
According to one of the major scientific goals of this mission, the Huygens probe managed a successful landing on its surface and it revealed extraordinary details of its structure and shape.
Although Cassini's observations are amazing, the evolution of the surface and its interaction with the lower atmosphere remain to be well identified. Obviously, only with an orbiter that will evolve around Titan and allow for long term observations of the Titan's surface, scientists can study in detail any tectonic processes and the existence and the evolution of the tectonic field. So long as the Cassini orbiter can only take snapshots of the surface, only test cases about tectonics can be assumed.
In this work, the Casini's radar image PIA09180 (Fig. 1) is studied by using geomorphologic methods, in order to find correlations between the surface features and the local tectonic field.

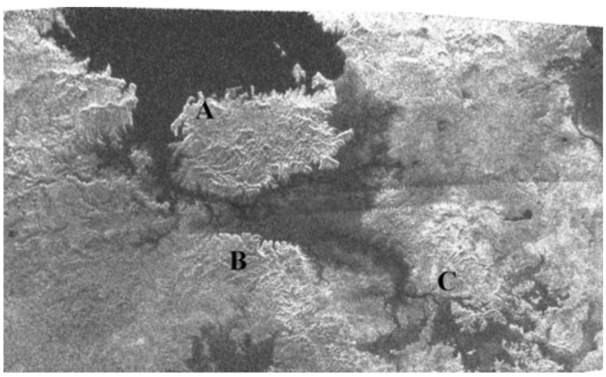

Fig. 1. Cassini's radar image PIA09180 (Credit: NASA/JPL).

The Cassini radar instrument took this image during its T25 flyby of Titan on February 22, 2007. It is a synthetic aperture (SAR) mode at a nominal resolution of 128 pixels/degree, which is approximately 351 m/pixel. The definition of ellipsoid for Titan is a sphere with radius 2575.0 km. This image is in an oblique cylindrical projection. In this geometry, the pixel spacing is exactly pi*2575/(180*128) = 0.35111 km in the direction of top to bottom. The coordinates of the center of this image are at about 79° N and 310° W. North is towards left.

Data obtained by a future mission to Titan with high-resolution images from a radar instrument will extend our knowledge for the formation of the surface and the active tectonics on Titan.

2. PHYSICAL GEOGRAPHY - OBSERVATIONS

The PIA09180 image (Fig. 1) shows a part of the Northern polar region of Titan, where the Cassini Radar instrument observed features like great lakes. The presence of hydrocarbon lakes on Titan was ascertained during the Cassini Radar flyby of Titan on 22 July 2006 [5, 7, 10].

Radar's transmitter sends out a microwave pulse and its receiver listens for that signal's echo, when it bounces back from the surface. Solid surfaces reflect better the radiation than liquid surfaces. The signal, after having been processed, determines the relative distance, position, and bearing of the reflected object. The radar dark patches on Titan are interpreted as lakes on the basis of their very low radar reflectivity and morphological similarities to lakes [10].

The gravity of Titan is 1.35 m/s^2, seven times lower than the Earth's and thus it is easier for mountains to occur. Few large impact craters are observed, so the surface must be young [2].

The most interesting feature in this image is an almost rectangular island or peninsula and its topography. North is to the left. A lake exists at the East part of the island.

At the West-Southwest side next to the island, a surface of low radar reflectivity exists. It is not as dark as the lake at the other side of the island and no significant topography is observed on it. A similar plateau is also observed at the South coast of the island, but not at the East. This area has an increased radar brightness compared to the lake. The same features have been previously observed at the edges of the lakes in Northern Titan and they might be due to a reflection from the lake bottom where it is sufficiently shallow that the bottom echo is not completely attenuated [10]. These features can be indicators of ground elevation.

The East and West coasts seem scarped and canyons in an average length of 20 km exist. Mountain ridges are extended to the coastline. The slopes are large and they have possibly tectonic origin. The region at the West has also topography with ridges. The Northern region seems to be smoother than the other regions.

The question is if the local topographic features are somehow related and if there is any evidence of tectonic activity in this region. Studying the development of the drainage system, we can bring constraints on the effects of the antecedent geological condition and subsequent geologic changes.

3. MORPHOLOGIC ANALYSIS

3.1 The Method

In order to understand the method we used, a step-by-step approach is required. Several classification systems have been proposed, in order to define the rule of the evolution of a drainage network. In this work we use the Horton and Strahler's ordering system [4, 8]. Horton's Laws are certain topological invariants that are needed to be satisfied. Horton's Laws connect the numbers and the lengths of streams of different orders in a drainage basin.

1) Law of Stream Numbers: The numbers of streams of different orders in a given drainage basin tend closely to approximate an inverse geometric series in which the first term is unity and the ratio is the bifurcation ratio.

2) Law of Stream Lengths: The average lengths of streams of each of the different orders in a drainage basin tend closely to approximate a direct geometric series in which the first term is the average length of streams of the first order [4].

Liquid flows form at high latitudes shallow rills. The lowest order streams, the rills, are the smallest outlying tributaries on the edges of the network, according to the Horton and Strahler's ordering scheme [4, 8]. At each point where two tributary streams join, a new stream originates. Whenever two tributaries of the same order meet, the outgoing stream has an order number one higher than that of the tributaries. If two tributaries of different orders meet, the outgoing stream has the same order number as the higher ordered tributary. Eventually, all streams in the network combine to form the highest order (main) stream.

The number of streams of order *u* is N_u, while $<L_u>$ is the average length of streams of order *u*. Horton's Laws [4] state that the bifurcation ratio R_b and the length ratio R_l, given by [4]

$$R_b = \frac{N_u}{N_{u+1}} \qquad (1)$$

$$R_L = \frac{< L_{u+1} >}{< L_u >} \qquad (2)$$

are constant, or independent of *u*.

3.2 Application and analysis

Fig. 2 shows the drainage classification of the island of the radar' s raster image PIA09180 (Fig. 1), according the Horton-Strahler's system [4, 8]. The unnumbered lines are the 1st order streams. The 2nd order streams are marked by the label "2" and 3rd order streams by the label "3". The basins' borders of the 3rd order streams are designed with thick dark lines and mentioned by roman numbers.

Since there is no topographic map with contour lines but only a radar image in greyscale, we have designed the streamlines following the fluctuation of the colours intensity. So, it is possible to find more streams, especially of the 1st order group in an image taken with higher resolution.

The Huygens probe measured the surface temperature at the landing area at 93.65 ± 0.25K, as reported by the Huygens Atmospheric Structure Instrument (HASI) [3], thus glaciers are expected. But the ice curtain is always shaped by the ground topography. The outlined drainage and its development can be used as a tool to study the evolution of the local surface.

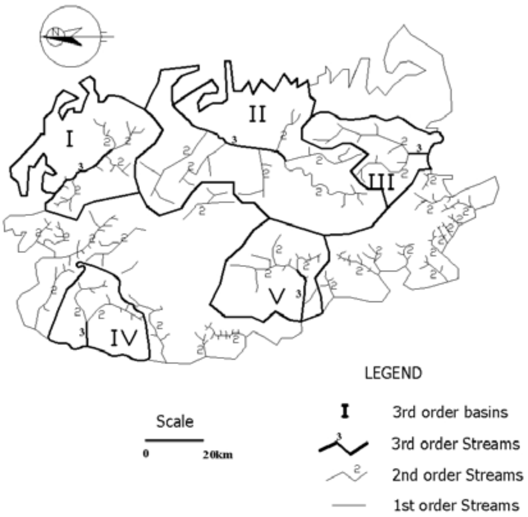

Fig. 2. The island's drainage (Cassini's Radar image PIA09180).

From the morphologic point of view the island can be divided in two different regions. The first contains the 3rd order basins labelled as IV, V, III and the second contains the basins labelled as II and I.

Table 1 contains the results of the analysis of the 3rd stream order basins, according the Horton-Strahler's classification system [4, 8] (Fig. 2).

The Bifurcation Ratio R_b is also calculated according the Eq. 1. Usually, the bifurcation ratio R_b has a range of 3 to 5 for well-drained networks. Numbers greater than 5 refer to deep and narrow basins [4].

Table 1 – Number of Streams formed the 3rd order basins of the island and Bifurcation Ratio

3rd order Basin	Stream Number				Bifurcation Ratio
	1st	2nd	3rd	TOTAL	
	N_1	N_2	N_3	ΣN_u	R_b
I	12	4	1	17	3.00
II	13	6	1	20	2.17
III	8	2	1	11	4.00
IV	8	2	1	11	4.00
V	11	2	1	14	5.50
TOTAL	52	16	5	73	

Table 2 contains the number of the streams of each order of the other two areas of the island where only 2nd order streams have been developed. We divide these streams in two groups, the North and the South, according the orientation of their flows. The last column of the Table 2 contains the total number of the streams of the entire island.

Table 2 – Streams of the island, which they do not belong to a 3rd order basin

Stream Order	North 2nd order Basins	South 2nd order Basins	Total Number of the streams of the island
1	37	37	126
2	9	12	37
3	0	0	5
Total	46	49	168

The total length of the streams in the 3rd order basins is listed in Table 3. L_u is the length value for each branch of the drainage system.

Table 3 –Lengths of the streams formed the 3rd order basins of the island

3rd order Basin	Stream Length			
	1st Order	2nd Order	3rd Order	TOTAL
	ΣL_1 (m)	ΣL_2 (m)	ΣL_3 (m)	ΣL_u (m)
I	38425.3	49287.3	25733.8	113446.5
II	76962.7	165799.5	45986.8	288749.0
III	32136.7	58416.1	6799.0	97351.8
IV	17857.3	49628.5	8456.5	75942.3
V	48650.1	36025.7	18827.3	103503.1
TOTAL	214032.2	359157.2	105803.4	678992.8

The average length of the Table 3 values is calculated in the Table 4 below, in order to find the length ratio R_L, according the Eq. 2.

Table 4 – Average length of the streams formed the 3rd order basins of the island

3rd order Basin	Average Stream Length		
	1st Order	2nd Order	3rd Order
	$\Sigma\langle L_1\rangle$ (m)	$\Sigma\langle L_2\rangle$ (m)	$\Sigma\langle L_3\rangle$ (m)
I	3202.1	12321.8	25733.8
II	5920.2	27633.3	45986.8
III	4017.1	29208.0	6799.0
IV	2232.2	24814.3	8456.5
V	4422.7	18012.9	18827.3

The stream length ratio R_L, the area A of each 3rd order basin and the Drainage Density D are listed in Table 5. The drainage density is calculated by the equation [4]:

$$D = \frac{\sum L}{A} \qquad (3)$$

Table 5 – Stream Length Ratio Area and Drainage Density of the 3rd order basins of the island

Stream 3rd order Basin	Stream length Ratio		Area of Basin	Drainage Density
	$R_L(2,1)$	$R_L(3,2)$	A ($x10^3$ km^2)	D (km^{-1})
I	3.8	2.1	1.35	0.08
II	4.7	1.7	2.96	0.10
III	7.3	0.2	0.76	0.13
IV	11.1	0.3	0.72	0.11
V	4.1	1.0	1.05	0.10
TOTAL			6.84	

Fig. 3 below shows the 2nd order basins of the Northern and Southern region of island, which do not have 3rd order streams developed in.

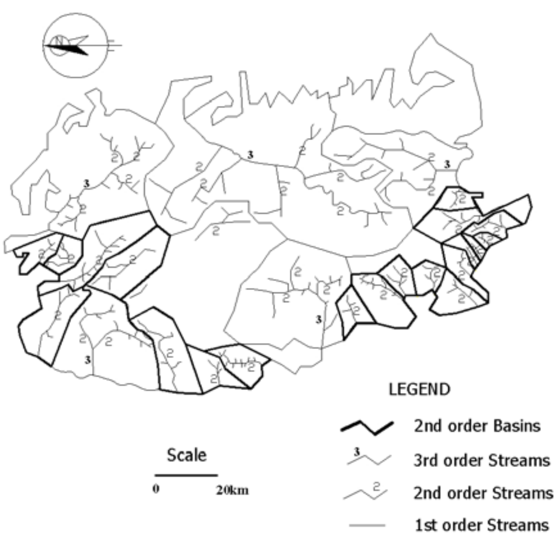

Fig. 3. 2nd order Northern and Southern basins.

4. CONCLUSIONS

The local surface isn’t homogenous and this can be caused by two factors, atmosphere and tectonic activity, operating separately or together. The role of the tectonic activity is to construct the surface and the role of the atmospheric phenomena is to reshape it.

Three main processes can produce surface liquid flows on Titan: (a) rainfall, (b) ice runoff, (c) subsurface deposits. The study of these processes will help us understand more about the operation of a possible methane cycle on Titan [1].

Tectonics gives the primary shape and structure of the surface, but processes like sediment erosion, transport and deposition and of course atmospheric phenomena sculpture the relief. During the time, liquid flows on a solid surface form rivers. The existence of the relief on a landscape can make a drainage network of rivers. Fluvial networks have been observed on Titan’ s surface [2]. Although the designed drainage (Fig. 2) seems to be dry it can operate and deploy on the island.

The purpose of the previous analysis is to study the evolution of the surface of the island and may think the existence of a local tectonic field. The Horton-Strahler analysis [4, 8] gives some evidence to this direction. Stream order affords a simple quantitative basis for composition of the degree of development. A basin is better drained as higher is the stream order.

First of all, the island’s area is approximately $12x10^3$km. It is obvious that the 3rd order basins cover more than half of the total area of the island as Table 5 shows. These basins have developed by 3rd order streams. This means that on the other half of the island a newly exposed surface exists, younger than the 3rd order basin’s relief.

The 3rd order basins I, II, IV, V cover almost the same area. Only the basin II is better drained and it is situated in the centre of the East part of the island. The other basins are deployed on the four corners of the island.

Because of the almost vertical entrance of the most tributaries into the main stream (Fig. 2), the drainage pattern can be described as rectangular.

The bifurcation ratio for the basin II is R_b =2.17, which means that the basin is well drained. The bifurcation ratio of the other 3rd order basins is greater than basin’s II due to their lower drainage development. Basin’s V ratio is greater than 5, which indicates a newly or elevated surface.

The stream length ratio R_L between 3rd order streams and 2nd order branches of the 3rd order basins is in a range of 0.2 to 2.1. Ratio R_L greater than 2 means that the 2nd order tributaries enter into the 3rd streams at acute angles, as do most streams on steeper slopes. The steeper the slope, the more acute is the angle of the stream entrance [4]. These basins are newly formed. Taking into account the stream length ratio R_L between 2nd order streams and 1st order branches, we can conclude that the 2nd order basins are newly formed during the drainage development.

The 2nd order streams of the well-drained basin II are long lengthened and deployed at the ¼ of the surface of the island. The longest 2nd order stream of this basin seems to be shaped like a meander, another clue of the well development of the basin II. The 3rd order streams of the basins III and IV are not well developed as the 2nd order streams, which they form them. The length each of the main 2nd order streams is equal to its drainage basin's length and it is greater than it originally would outlined have been for a drainage basin of the same order of normal form. Moreover, 2nd order basins are poorly drained. This indicates that the basins are fixed by geology.

The island's drainage is thin. The drainage density *D*, listed in Table 5, extends to zero, although there is a considerable degree of basin development. This can be explained by the existence of intermittent and ephemeral streams in the region [4] and of course by the low image resolution.

The 1st order streams flow parallel or are consequent on the original slope of the surface. These rills are steep-sided, have short lengths and are V-shaped. The number of these streams (52), as Table 2 shows, is greater than the numbers of the streams of the 2nd (16) and 3rd (5) order at the 3rd order basins I, II, IV, V.

This is because the surface in these regions is newly exposed and basin II is the only one well drained. To summarize the results of the drainage network analysis, we find that (a) the 3rd order basins I, II, IV, V and the Northern and Southern 2nd order basins are situated in newly exposed or elevated surfaces, (b) basin II is well drained and relatively well developed. ***There is evidence of local tectonic activity, which affected the island's topography.***

5. ANGULAR DISTRIBUTION OF THE MOUNTAIN RIDGES

Three regions with significant topography are observed in the Cassini's Radar image (PIA01980), mentioned with A, B, C in Fig. 1. In Tables 6,7 and 8 below, are listed the angles in degrees, which show the orientation of the axis of the mountain ridges, according to the N-S direction.

Table 6. Angles of mountain ridges according the N-S direction, Region A - The Island

Angles (deg) of the main Mountain Ridges of Region A – Island								
41.7	-5.6	6.6	-7.3	30.6	2.7	-47.8	71.4	19.4
39.5	-6.1	-12.2	-19.6	-10.0	42.9	-42.5	-2.2	22.8
41.4	20.5	-16.4	38.6	-30.1	39.0	39.9	-14.2	16.6
14.8	-8.7	26.4	27.3	-54.4	-0.5	59.4	-21.5	-25.9
-27.2	41.0	-11.7	46.3	52.1	-10.1	-0.1	34.8	21.1
12.1	-19.7	-19.1	-19.1	-30.9	-47.4	-18.7	-3.2	62.1
44.6	-6.5	15.9	-22.4	-23.9	-3.7			

Table 7. Angles of mountain ridges according the N-S direction, Region B - Western Mountains

Angles (deg) of the main Mountain Ridges of Region B – Western Mountains								
20.8	13.7	-20.6	-5.8	20.8	53.1	-47.5	31.6	-30.5
7.5	30.7	43.7	-27.1	8.1	-19.0	-34.8	-5.2	-8.7
65.3	32.8	53.3	-10.6	70.2	47.0	14.5	25.7	24.4
30.4	-45.0	-2.7	36.2	-54.7	-2.9	-24.0	51.3	28.7
-58.2	-37.9	-27.0	12.8	38.3	0.0	-22.1	25.0	20.8
43.9	72.2	35.8	32.6	5.3	-17.3	-2.3		

Table 8. Angles of mountain ridges according the N-S direction, Region C - SW Mountains

Angles (deg) of the main Mountain Ridges of Region C- SW Mountains				
-3.5	-39.9	30.3	16.7	0.0
16.1	8.3	47.1	12.8	16.7
51.4	54.1	13.8	0.0	22.1
40.9	-9.8	-57.1	11.0	-46.0
33.3	-39.9	44.1	35.3	-33.7
9.5				

The angle distributions of the mountain ridges' orientations are presented in Figs. 4, 5 and 6. The positive angles are looking to the East and the negatives to the West. The normal curve is also included.

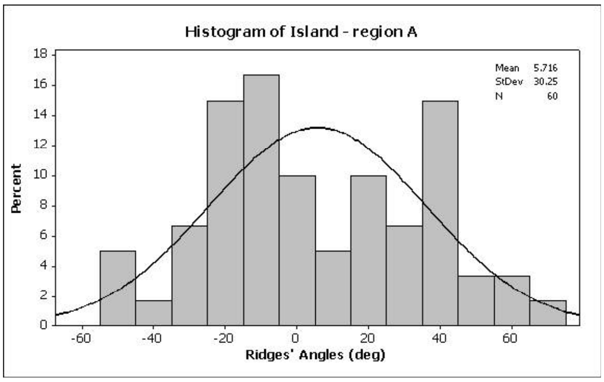

Fig. 4. Histogram of the Island-region A

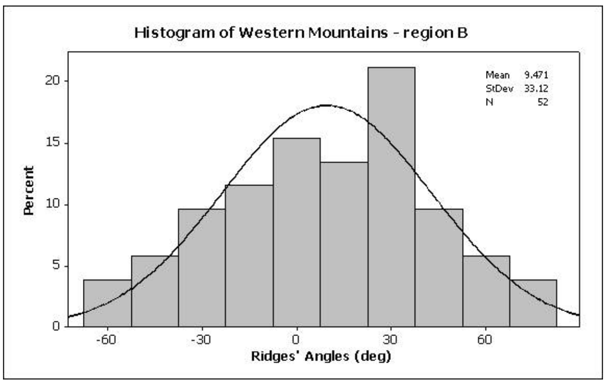

Fig. 5. Histogram of the Western Mountains-region B

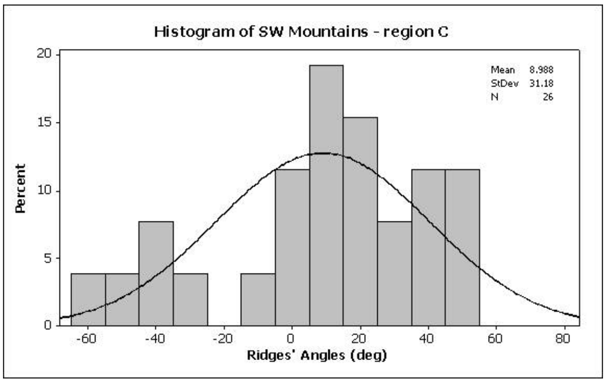

Fig. 6. Histogram of the SW Mountains-region C.

Interesting results are concluded by histograms showed in Fig. 4, 5 and 6. The angle distribution of the mountain ridges has a specific N-E orientation at a range of 10^o to 20^o at the S-W Mountains, 30^o at the Western Mountains and 20^o and 40^o at the island. This might be evidence of the same tectonic mechanism operated to create this topography.

The next interesting result of this preliminary analysis is that at the region A an opposite orientation exists. There are almost 30% of the ridges that are N-W oriented. A recent tectonic process can be assumed, which change the prime N-E orientation of the mountains. Due to the low radar resolution, only a sample of the mountain ridges is examined. A high-resolution image will provide the accurate orientation of the ridges.

6. ANGULAR DISTRIBUTION OF THE ISLAND'S 2nd ORDER STREAMS IN POOR DRAINED BASINS

As we observed above, there are in the Island 2nd order streams poorly drained (Fig. 3). At the remaining region of the island, except the 3rd order basins, the 2nd order streams have been developed vertical the coastline. The orientation of these streams, according to the N-S direction, is listed in Table 9 below.

Table 9. 2nd Order Stream Angles Orientation according to N-S direction

2nd Order Stream Angles (deg) to N-S direction			
83.7	-67.1	-56.7	-72.5
55.7	67.9	-39.8	-72.5
22.9	-42.1	4.5	-88.2
27.3	-72.3	11.3	31.9
55.6	-59.6	61.0	-26.7

The angle distribution of Table 9 is designed in Fig. 7, with the normal curve.

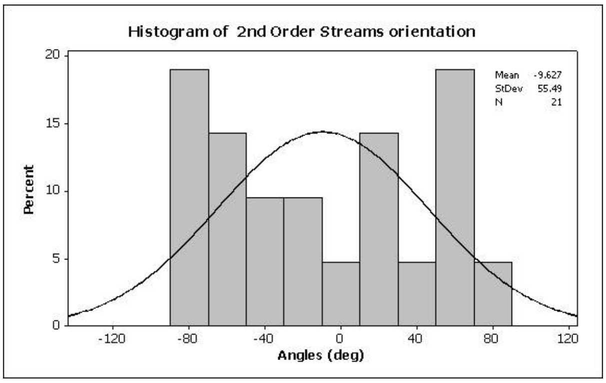

Fig. 7. Histogram of 2nd order Streams orientation of Northern and Southern poor drained basins.

The Northern streams are N-W oriented and the Southern streams are N-E oriented. Comparing the two histograms of the Island (Fig. 4 and Fig. 7), the streams in poorly drained regions seems to be consequent on the axis of the mountain ridges of the surface. This is also an indicator of a newly exposed surface, because the degree of the stream erosion and the basin development is not as adequate as at the neighbor basins. Probably, they are fixed after the surface elevation caused by the local tectonic activity.

7. DETERMINATION OF THE LOCAL TECTONIC FIELD

Cassini-Huygens mission reveals new frontiers for Science. In order to explain new observations, scientists have to consider what physical and chemical processes occur on Titan. One of the major questions concerning Titan is if the moon is tectonically active or not. To answer this question, data obtained by a Titan orbiter needed. Evidences of tectonic activity have been proposed on Titan [9].

However, by studying Cassini's images, we can assume the local events have occurred. After having analyzed the Cassini's Radar image PIA09180 topography, interesting results are concluded.

To summarize the previous analysis, (1) the relief of the image is smoother at the East side of the Island than at the other side. Thus, we can divide the region in two parts, the East and the West. The smooth relief provides terrain movements downwards. The West part includes features like mountain ridges, a canyon, scarp coastline and a shallow plateau. These features can be indicators of upward ground elevation. (2) The development of the Island's drainage network is quite different between the two parts. At the Eastern part is well drained, containing 3rd order lengthen streams and meander branches and forming a large area basin. The Western part is poorly drained without 3rd order streams or if those streams exist are short lengthen in relation with the 2nd order branches. This obviously resulted by tectonic processes. (3) The deployment of the 2nd order basins and the length of their main streams, which is equal to the basin's length, provide that they are fixed by geological structures. In addition, the 2nd order basins and their main streams are oriented towards the local relief. The mountain ridges orientation of the entire region shows a correspondence of the topography to a former process, which happened before the deployment of the drainage. A newly tectonic process must have occurred, in order to regenerate the Island's shape. To determine how long ago the newly tectonic activity occurred, detailed *in situ* measurements of the entire area are needed.

Newly tectonic activity is not occurred the same way at the entire island. Besides the downward movement of the East part of the Island due to drainage development, the result of the newly tectonic process is the elevation of the West part. Thus the drainage network of the Western part has been changed.

The local tectonic field is consisted by two concurrent forces, which compressed the Island from opposite sides. One acted on the N-W side of the Island and the other on S-W part. These forces elevated the West part of the Island. More specific description of the local tectonic field will be provided in future if radar images in high-resolution obtained.

8. INSTRUMENTATION FOR FUTURE MISSION

The Cassini radar instrument takes 4 types of observations: imaging, altimetry, backscatter and radiometry. This instrument is based on the same technology used in Magellan mission to Venus and the Earth orbiting Space borne imaging radar.

Cassini's observations revealed a complicated surface on Saturn's larger moon. By the end of the planned mission, however, Cassini's radar will have covered only 15% of Titan's surface, and its Visual and Infrared Mapping Spectrometer just a few percent, at a resolution of less than a km per pixel (Sotin, et al, 2007).

To study Titan's surface and outline a detailed topographic map of its globe, radar images in high-resolution needed. This project can be accomplished from a stable Titan orbit remote sensing package on a future orbiter. Thus, the evolution of the surface and the interaction with the lower atmosphere will be identified. Radar instrumentation is considered as a payload to a future mission (TANDEM, in response to ESA's Cosmic Vision Call 2015-2025: http//despa.cosmicvision/tandem).

Issues for further research from the data obtained by high-resolution radar images are: (1) to determine if the tectonic forces are still in action, (2) evaluate the age of Titan's surface, (3) discover the composition and the source of the lake liquid, (4) measurements of the lakes' depths, (5) uncover the relation between the surface lithology and the surface features.

Studying Titan is like studying a prime Earth-like environment and discovering Titan's mysteries will help us study the origins of our own planet.

Acknowledgements:

The Cassin's radar image PIA09180 is provided from NASA/JPL. We thank Dr. Randolph L. Kirk for fruitful discussion. We also thank the Chair and the Members of the IPPW5 Student Programme Committee for the finantial support in order to attend the IPPW5.

REFERENCES

1. Atreya S. K. et al., Titan's methane cycle, *PLANET. SPACE SCI.*, Vol. 54, 1177-1187, 2006.

2. Elachi, C., et al., Cassini Radar Views the Surface of Titan, *SCIENCE*, Vol. 308, no. 5724, 970–974, 2005.

3. Fulchignoni M. et al. *In situ* measurements of the physical characteristics of Titan's environment, *NATURE*, 438, 785-791, 2005.

4. Horton, R. E. Erosional development of streams and their drainage basins; Hydrophysical approach to quantitative morphology, *GEOL. SOC. AMERICA BULL.*, 56, 275-370, 1945

5. Mitri, G., et al., Hydrocarbon lakes on Titan, *ICARUS*, Vol. 186, 385-394, 2007.

6. Lorenz, R. D., et al. The Sand Seas of Titan: Cassini RADAR Observations of Longitudinal Dunes, *SCIENCE*, Vol. 312, no. 5774, 724-727, 2006.

7. Sotin, C., et al. Titan's lost seas found, *NATURE*, 445, 61-64, 2007.

8. Strahler, A. N., Hypsometric (area-altitude) analysis of the erosional topography, *GEOL. SOC. AMERICA BULL.*, v. 63, 1117-1142, 1952.

9. Stofan, E. R., et al., Mapping of Titan: Results from the first Titan radar passes, *ICARUS*, Vol. 185, no. 2, 443-456, 2006.

10. Stofan, E. R., et al. The lakes of Titan, *NATURE*, 445, 29-30, 2007.

11. Tomasko M.G., et al. Rain, winds and haze during the Huygens probe's descent to Titan's surface, *NATURE*, 438, 765-778, 2005.

12. Zarnecki J. C., et al. A soft solid surface on Titan as revealed by the Huygens SurfaceScience Package, *NATURE*, 438, 792-795, 2005.